International Geology Review, Vol. 38, 1996, p. 389–404.

Archean Enriched Mantle Beneath the Baltic Shield: Rare-Earth-Element Evidence from the Burakovsky Layered Intrusion, Southern Karelia, Russia

GREGORY A. SNYDER, STEFAN J. HIGGINS, LAWRENCE A. TAYLOR,

Planetary Geosciences Institute, Department of Geological Sciences, University of Tennessee, Knoxville, Tennessee 37996

JINESH JAIN, CLIVE R. NEAL,

Department of Civil Engineering and Geological Sciences, University of Notre Dame, Notre Dame, Indiana 46556

AND EVGENII SHARKOV

Institute of Ore Deposit Geology, Petrology, Mineralogy, and Geochemistry, Russian Academy of Sciences, Moscow 109017, Russia

Abstract

In order to better understand the origin and character of late-Archean mantle beneath the Baltic Shield, we have analyzed mafic-ultramafic rocks from one of the best-preserved, least-metamorphosed regions of Karelia, Russia. Trace-element data for samples from the ultramafic and gabbronorite zones of the large (700 km²) Burakovsky layered intrusion (BLI) are presented. Samples from the ultramafic zone are LREE enriched, indicating that they formed from a LREE-enriched parental magma. Indeed, a calculated parental magma for the ultramafic zone has a $(Ce/Yb)_n$ ratio of 2.6, a $(Nd/Sm)_n$ ratio of 1.1, and a $(Dy/Yb)_n$ ratio of 1.6. The LREE enrichment in the parental magma suggests either that the source region was LREE enriched or that the melt was contaminated by crust en route to the BLI magma chamber. Samples from the gabbronorite zone also are LREE enriched and indicate two distinct parental magmas. Group-I magmas, from the lower part of the gabbronorite zone, have $(Ce/Yb)_n$ ratios of 6.9 to 13.9, whereas Group-II magmas, from the upper portion, have $(Ce/Yb)_n$ ratios of 15.8 to 27.3. Volcanic rocks in Karelia that are coeval to the Burakovsky layered intrusion, as well as volcanic rocks of a similar age in other parts of the Baltic Shield, also are LREE enriched. Furthermore, the BLI has an initial ϵ_{Nd} value of −2.0, and other layered intrusions in the Baltic Shield of similar age also have negative initial ϵ_{Nd} values (e.g., −1.8 to −2.2). The consistency of these ϵ_{Nd} values for layered intrusions throughout Karelia precludes contamination as a controlling factor in their isotopic compositions. All of these data are most consistent with the development of LREE-enriched mantle beneath the eastern Baltic Shield, prior to the earliest Proterozoic.

Introduction

IT HAS LONG BEEN DEBATED whether the Archean/Proterozoic transition worldwide represents an important, fundamental change in tectonic style, melting of the mantle, and crustal evolution. Rift-related magmatism within these preserved Archean crustal segments during the earliest Proterozoic provides a unique view into the mantle, the degree of melting, an estimate of its composition, and its division into various geochemical domains. Furthermore, comparison of the character of earliest Proterozoic magmatism with that in the Archean should allow us to evaluate various hypotheses of evolution of these mantle domains. Source regions that are enriched in incompatible elements over a chondritic bulk Earth are common in the present-day mantle (Menzies, 1990). However, it still is not known how widespread such enriched-mantle sources were in the early Earth. Enriched mantle of Archean age has been suggested beneath southern Africa (e.g., Menzies and Murthy, 1980; Richardson et al., 1985), the Wyoming province of the United States (e.g., Carlson and Irving, 1994; O'Brien et al., 1995), and Greenland (e.g., Scott-Smith, 1987). Recently, Balashov et al. (1993) and Amelin et al. (1995) have considered that the isotopic compositions of mafic intrusions in the eastern Baltic Shield are the

0020-6814/96/187/389-16 $10.00

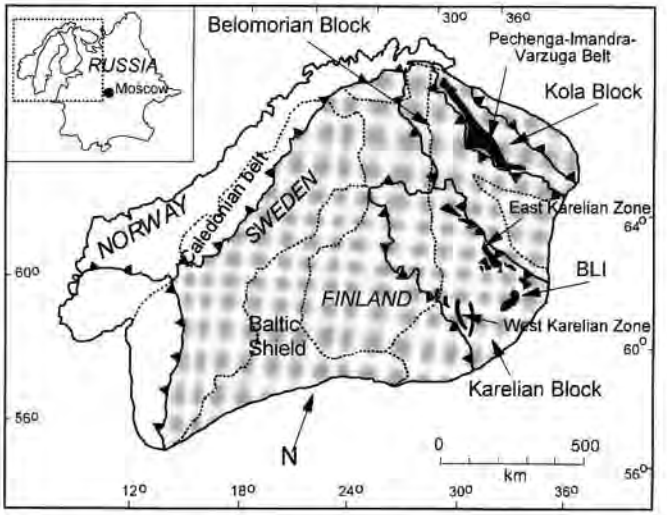

FIG. 1. Simplified tectonic map of the Baltic Shield. Major tectonic blocks are defined by lines with triangles. Boundaries of countries within the shield are designated by dashed lines. The two major supracrustal belts in the eastern Baltic Shield—the Pechenga-Imandra-Varzuga belt and the Karelian belt (subdivided into the West and East Zones)—also are shown. The inset in the upper left corner shows (from left to right) Norway, Sweden, Finland, and western Russia and the location of the map area (outlined by dashed lines). Abbreviation: BLI = Burakovsky layered intrusion.

result of either: (1) extensive crustal contamination of mantle-derived magmas or (2) direct derivation from enriched mantle. We are currently evaluating these two hypotheses by looking at the trace-element chemistry of early Proterozoic layered mafic intrusions and associated volcanics in western Russia.

The Baltic Shield, a large Archean crustal segment that consists of a granite-greenstone belt to the south and various cratonic masses separated by mobile belts to the north, extends from present-day southern Norway, through Sweden and Finland, and into western Russia all the way to the Arctic Ocean (Gorbatschev and Bogdanova, 1993) (Fig. 1). These Archean cratonic masses probably were brought together sometime in the late Archean, and, soon thereafter, rifting first began. This rifting is evidenced by both volcanic rocks and layered mafic intrusions, which have yielded ages in the earliest Proterozoic (Balashov et al., 1993; Mitrofanov and Torokhov, 1994; Amelin et al., 1995). Nearly 30 mafic plutons of early Proterozoic age are located within the Baltic Shield (Alapieti et al., 1990). These intrusions lie within two separate volcanic-sedimentary belts, the northern Pechenga-Imandra-Varzuga belt on the Kola Peninsula and the southern Sumi-Sariola belt of Karelia (Fig. 1). Magmatism in the southern belt spanned a very narrow age range, from 2441 to 2449 Ma (Amelin et al., 1995). The oldest intrusion in this southern belt and, thus, the earliest magmatic event, is the Burakovsky layered intrusion (2449.0 ± 1.1 Ma).

The Burakovsky layered intrusion is unique in many aspects and affords the best opportunity to study mantle-derived, rift-related magmatism in the earliest Proterozoic. It is the largest mafic pluton in all of Europe (Alapieti et al., 1990). Thus, it represents a major and voluminous magmatic episode in the early Proterozoic. The Burakovsky layered intrusion also is the most primitive intrusion in the southern

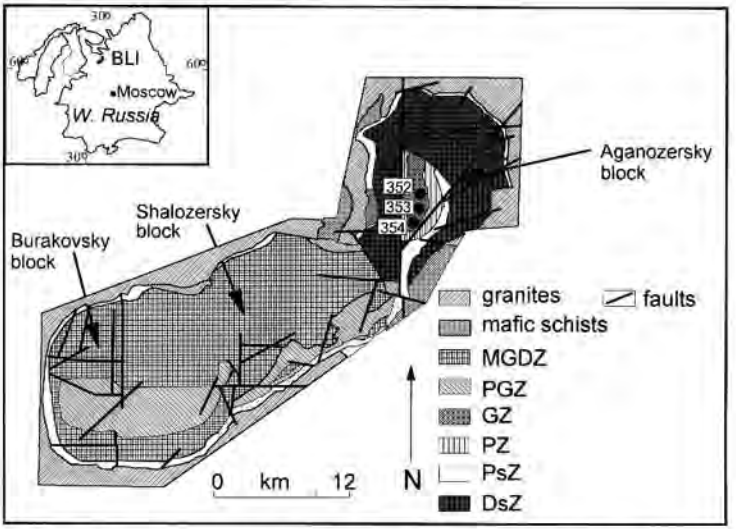

FIG. 2. A simplified geologic map of the Burakovsky layered intrusion with major faults (dividing the major structural blocks) shown by solid lines. The inset indicates the location of the Burakovsky layered intrusion (BLI) relative to the city of Moscow. Drill cores 352, 353, and 354 are indicated by filled circles. Abbreviations: MGDZ = magnetite-gabbrodiorite zone; PGZ = pigeonite-gabbronorite zone; GZ = gabbronorite zone; PZ = pyroxenite zone; PsZ = peridotite subzone; DsZ = dunite subzone.

Sumi-Sariola belt and, indeed, in all of western Russia. Whereas other major layered intrusions have bulk compositions with Mg#s [atomic Mg/(Mg + Fe)] of 58 to 79 and MgO contents from 8.2 wt% to 17.9 wt%, the Burakovsky intrusion is much more primitive, with an Mg# of 84, MgO content of 29.3 wt%, and the lowest K content of any major intrusion (Koptev-Dvornikov, 1995). Furthermore, the Vodlozero block, the Archean segment that contains the Burakovsky intrusion, is unlike the rest of the eastern Baltic Shield in that it has not experienced a regional metamorphic event since the latest Archean (Amelin et al., 1995). Therefore, the Burakovsky intrusion is unique among layered intrusions of the Baltic Shield in that it has not been metamorphosed by any regional event. Finally, abundant komatiitic volcanic rocks of similar bulk composition and age are found associated with the Burakovsky layered intrusion (Bogatchikov, 1988). Thus, the Burakovsky intrusion has preserved the most voluminous, least metamorphosed, most uncontaminated, and least differentiated (from a mantle-melt composition) magmas found in the eastern Baltic Shield. Indeed, the Burakovsky intrusion and associated volcanics are the best point of departure for a study of mantle chemistry, melting, and differentiation during earliest rifting of an Archean craton.

Early Proterozoic magmatism in the Baltic Shield, best represented by rocks of the Burakovsky layered intrusion, may not be simply a regional event. Alapieti et al. (1990) have speculated that early Proterozoic magmatism in the Baltic Shield may have been part of a global early Proterozoic event that included the Jimberlana intrusion of Australia (2420 ± 30 Ma) (McClay and Campbell, 1976), the Great Dyke of Zimbabwe (2461 ± 16 Ma) (Wilson and Prendergast, 1987), the Scourie dikes of Scotland (2418 ± 7 Ma) (Heaman and Tarney, 1989), the Hearst-Matachewan dike swarm and the East Bull Lake gabbro in Canada (2452 ± 3 Ma and 2480 ± 10 Ma, respectively) (Krogh et al., 1984; Heaman, 1988), and the Vestfold Hills and Napier complex dikes of Antarctica (2424 ± 72 Ma and 2350 ± 48 Ma, respectively)

(Sheraton and Black, 1981; Collerson and Sheraton, 1986). Thus, a study of the Burakovsky intrusion and associated komatiitic volcanics could further our understanding of mantle chemistry and its lateral variation during this major worldwide magmatic episode.

Geology of the Burakovsky Layered Intrusion

The 700-km² Burakovsky layered intrusion (BLI) of southern Karelia, Russia is the largest mafic pluton in the Baltic Shield. It lies within the E-W-trending Finno-Karelian supracrustal belt and is associated with the most prominent suture zone on the Baltic Shield, the East Karelian (Fig. 1). U-Pb dating of zircons indicates an age of 2449 ± 1.1 Ma for the BLI (Amelin et al., 1995), consistent with the idea that the BLI and other layered intrusions of the Baltic Shield formed as a result of intrusive igneous activity that occurred between 2.4 and 2.5 Ga. Emplacement of these layered intrusions occurred as two distinct magmatic episodes at 2505 to 2501 Ma in the Kola Peninsula and 2449 to 2441 Ma in Karelia and the Kola Peninsula (Amelin et al., 1995). Intrusions that mark the first event include the Monchegorsk and Pana Tundra plutons (2504.4 ± 1.5 Ma and 2501.5 ± 1.7 Ma, respectively). The second magmatic event is evidenced by such plutons as the Burakovsky of southern Karelia and the Lukkulaisvaara (2442.1 ± 1.4 Ma) and Tsipringa (2441.3 ± 1.2 Ma) intrusions of the Olanga complex in northern Karelia (Fig. 1). Both of these events are related to continental rifting in zones of pre-existing lithospheric weaknesses (Amelin et al., 1995).

The lithology of the BLI is dominated by layered ultramafic and mafic rocks, and it has been divided into three major blocks by faults—the Aganozersky, the Shalozersky, and the Burakovsky (Fig. 2). An extensive description of the mineralogy, petrology, and structure of this intrusion is presented in Sharkov et al. (1995) and Higgins et al. (1997). These authors recognized five major stratigraphic subdivisions in the BLI. From the bottom upward these are: (1) an ultramafic zone, consisting of 2.6 km of dunites overlain by 0.4 km of peridotites; (2) a pyroxenite zone, consisting of 0.2 km of clinopyroxenites; (3) a gabbronorite zone, consisting of a 0.7-km-thick, lower banded subzone of alternating plagioclase-rich and olivine/pyroxene-rich cumulates and a 0.32-km-thick, upper anorthosite subzone; (4) a 1.2-km pigeonite-gabbronorite zone; and (5) a 0.8-km magnetite-gabbrodiorite zone (Fig. 2).

Sampling and Analytical Methods

Whole-rock trace-element analyses were performed on 15 samples from several drill cores penetrating the gabbronorite and ultramafic zones of the BLI. Of the samples analyzed, two were from the ultramafic zone and one was from the border group. Samples are labeled using core number and depth in meters (e.g., core #/depth). An extensive major-element study was conducted on samples from drill cores 353 and 354, and these results are presented in Higgins (1996) and Higgins et al. (1997). In this paper, we also have included trace-element analyses for samples from one other core (352), but the bulk of the data are for cores 353 and 354.

Trace-element concentrations for samples from the ultramafic zone and the gabbronorite zone were determined with a FISONS-VG PlasmaQuad II STE Inductively Coupled Plasma Mass Spectrometer at the University of Notre Dame. Detection limits for most elements that we are interested in—e.g., the rare-earth elements (REE), Co, Ni, Cr, Hf, Li, and Ba—are in the parts per billion (ppb) range. These detection limits (in ppb) are as follows: (1) Sc = 0.054; (2) V = 0.113; (3) Cr = 0.105; (4) Co = 0.005; (5) Ni = 0.008; (6) Cu = 0.206; (7) Rb = 0.150; (8) Sr = 0.207; (9) Y = 0.003; (10) Zr = 0.018; (11) Nb = 0.003; (12) Ba = 0.041; (13) REE = 0.03 to 0.024; (14) Hf = 0.011.

Results

The analytical results for samples from the ultramafic zone are presented in Table 1; major-element data for these samples can be found in Higgins et al. (1997). Chondrite-normalized REE plots of these data appear in Figure 3. In general, all of the samples have negative slopes and are enriched in light rare-earth elements (LREE). This suggests that the parental magma for these samples also was LREE enriched.

Whole-rock trace-element abundances (in ppm) for samples from the gabbronorite zone

TABLE 1. Whole-Rock Trace-Element Abundances (ppm), Selected Samples, Ultramafic Zone[1]

Element	248/190	200/444	28/223[2]	Cal. parent
Sc	22.2	12.7	11.2	13.9
V	72.7	49.9	76.8	103.7
Cr	3379.1	6915.5	3744.4	2431.4
Co	104.8	102.1	124.9	60.0
Ni	1461.7	2359.4	1947.7	220.6
Cu	23.1	221.7	84.3	107
Rb	0.34	0.07	8.3	11.4
Sr	26.8	13.7	81.2	7.63
Y	3.04	1.79	5.61	7.63
Zr	6.96	2.8	40.4	55
Nb	0.27	0.1	1.88	2.58
Ba	3.03	8.12	115.7	36.8
La	0.92	0.49	5.8	2.22
Ce	2.4	1.39	13.2	6.31
Nd	1.76	1.02	6.64	4.63
Sm	0.54	0.3	1.47	1.36
Eu	0.17	0.1	0.39	0.45
Gd	0.53	0.31	1.27	1.74
Tb	0.09	0.05	0.2	0.27
Dy	0.6	0.33	1.13	1.55
Ho	0.11	0.07	0.2	0.27
Er	0.31	0.17	0.54	0.74
Tm	0.04	0.02	0.06	0.08
Yb	0.25	0.16	0.47	0.64
Lu	0.03	0.02	0.06	0.08
Hf	0.19	0.11	1.05	1.43

[1]Included are the trace-element concentrations in a calculated parent for this zone.
[2]Sample from the border group.

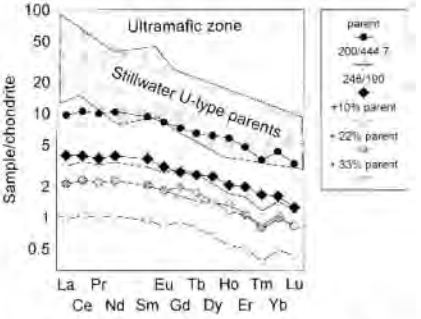

FIG. 3. REE plot for two samples (open and closed diamonds) from the ultramafic zone, normalized to the CI chondrites (Wasson and Kallemeyn, 1988). Also shown is the calculated parent liquid for the ultramafic zone (see text) as well as mixtures of a model dunite cumulate with varied proportions of trapped parental liquid (10%, 22%, and 33%). A field representing U-type parental magmas for the ultramafic series of the Stillwater complex is shown for comparison (after Papike et al., 1995). Data are presented in Table 1.

are presented in Table 2. Again, the major-element data for these same samples are given in Higgins et al. (1997). The REE abundances, normalized to chondritic meteorites, are shown in Figure 4. As with the ultramafic zone, all of the samples are LREE enriched and depleted in the heavy rare-earth elements (HREE). Moreover, most of the samples have positive Eu anomalies, which reflects the presence of plagioclase. Note that sample 353/140 has anomalously low HREE values and that sample 354/279 is strongly depleted in the LREE relative to the other samples. This may suggest contamination, or, in the case of sample 354/279, formation from an ultramafic magma. These ideas will be considered in detail in the ensuing discussion.

Parental Magma Characteristics

A major problem in modeling REE abundances in cumulus rocks and minerals concerns the calculation of the parent-magma composition (e.g., Wager and Deer, 1939). In particular, this is difficult when working with adcumulates in which no intercumulus phases remain representative of the parental magma. Indeed, even in orthocumulates, the interstitial minerals probably do not truly reflect the closed-system crystallization of trapped intercumulus liquid (Irvine, 1980). One way around this problem is through use of a basal chill margin to estimate the parental magma characteristics (Wager and Deer, 1939). Theoretical modeling of REE partitioning in orthopyroxene and plagioclase (Simmons and Lambert, 1982) has demonstrated that cores of cumulus minerals may be used to estimate parental magma characteristics. Of course, this requires knowledge of the trace-element abundances in individual minerals, and these data are not always available. In fact, as with the current study, whole-rock trace-element abundances often are the only available means for estimating the parent compositions. Regardless of the method employed, these data, when combined with mineral-melt partition coefficients (D values), provide important clues concerning the chemistry of

TABLE 2. Whole-Rock Trace-Element Abundances (ppm), Selected Samples, Gabbronorite Zone

Element	353/60	353/94	353/140	353/160	354/172	354/207	354/215	354/245	354/279	353/397	352/172	352/177
Sc	17.9	34.1	3.03	17.7	22.7	35.0	16.6	23.3	39.2	11.4	35.8	37.5
V	118.7	190.0	18.4	84.5	105.2	162.0	73.7	107.3	154.1	41.1	170.7	170.1
Cr	120.0	1510.0	27.6	103.0	317.8	924.7	541.7	3093.6	2974.7	466.5	1554.0	2943.6
Co	42.5	57.3	16.3	37.5	160.0	187.2	201.7	210.1	121.9	27.8	59.3	74.6
Ni	204.6	226.3	90.0	230.3	239.3	574.8	222.7	626.8	735.3	173.5	460.6	575.0
Cu	572.9	245.3	137.2	117.7	89.7	188.1	64.8	152.8	57.8	61.5	36.2	44.2
Rb	10.9	5.32	15.1	6.81	1.55	1.30	0.88	1.81	0.32	2.02	26.2	1.47
Sr	451.1	287.4	558.3	419.8	501.4	63.2	613.7	116.7	43.7	720.4	123.0	56.1
Y	6.25	8.15	2.03	3.41	3.77	5.98	2.49	3.58	4.62	2.04	9.68	5.57
Zr	31.0	24.8	127.2	15.4	8.06	18.7	4.46	10.6	4.69	4.17	70.2	10.4
Nb	1.68	0.81	2.08	0.80	2.63	3.68	6.55	3.84	1.78	0.16	5.04	0.17
Ba	180.6	109.9	207.2	116.4	52.5	18.0	45.3	55.2	6.00	51.5	83.3	15.6
La	5.59	4.08	6.09	3.40	1.43	1.76	0.92	1.51	0.48	1.20	40.5	2.0
Ce	12.1	9.58	11.6	6.77	3.46	4.58	2.05	3.57	1.77	2.74	23.1	5.59
Nd	5.31	5.49	3.82	2.97	2.30	3.29	1.43	2.31	2.00	1.60	10.0	3.11
Sm	1.19	1.44	0.59	0.65	0.67	0.97	0.42	0.60	0.76	0.41	2.17	0.87
Eu	0.57	0.52	0.50	0.38	0.36	0.26	0.27	0.24	0.25	0.27	0.58	0.26
Gd	1.22	1.48	0.57	0.65	0.71	1.03	0.47	0.59	0.81	0.40	1.99	0.86
Tb	0.20	0.25	0.06	0.10	0.12	0.19	0.07	0.10	0.16	0.06	0.34	0.16
Dy	1.22	1.61	0.38	0.63	0.76	1.18	0.47	0.68	1.00	0.38	2.03	1.06
Ho	0.22	0.30	0.07	0.12	0.14	0.21	0.09	0.13	0.18	0.07	0.37	0.19
Er	0.62	0.86	0.19	0.33	0.37	0.63	0.26	0.36	0.48	0.20	0.97	0.53
Tm	0.08	0.12	0.02	0.04	0.05	0.09	0.05	0.05	0.06	0.03	0.14	0.08
Yb	0.56	0.76	0.15	0.32	0.35	0.56	0.23	0.38	0.39	0.16	0.87	0.51
Lu	0.08	0.10	0.02	0.04	0.04	0.08	0.02	0.05	0.05	0.01	0.11	0.07
Hf	0.86	0.74	2.65	0.41	0.26	0.54	0.15	0.30	0.23	0.12	1.98	0.32

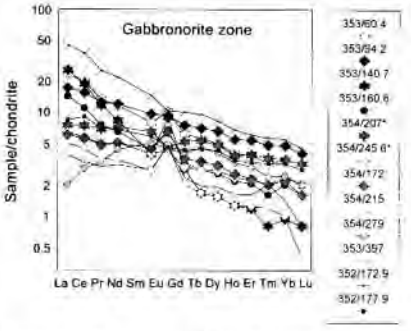

FIG. 4. REE plot normalized to CI chondrites (Wasson and Kallemeyn, 1988) for 12 samples from the gabbronorite zone. All samples but one (354/279) indicate LREE enrichment.

the liquid from which the various cumulates crystallized. Table 3 summarizes the partition coefficients used in this study.

Calculated parental liquid for the ultramafic zone

Major-element modeling with the program MAGFOX (John Longhi, pers. commun.) indicates that the border group of the BLI represents a chilled margin of the ultramafic zone (Higgins et al., 1997). On the basis of phase relations, however, this sample is too enriched in Mg relative to Fe to qualify as a parental magma (i.e., $X_{Mg} = 0.78$, where X_{Mg} is defined as Mg/(Mg+Fe)). Therefore, it was necessary to recalculate the parental liquid for the ultramafic zone using a mass-balance approach. In this calculation, we assumed that the liquid composition represented by the border-group sample contained excessive olivine of a relatively primitive composition (i.e., the olivine was assumed to have an X_{Mg} value of 0.87, which equals the most primitive olivine analyzed in this study). In order to produce an X_{Mg} of 0.72, the maximum allowed by mantle-relevant phase relations, it was necessary to remove 27% of this primitive olivine from the matrix. A similar mass balance approach was used to recalculate the trace-element concentrations. Table 1 presents the trace-element abundances of the border-group sample and the calculated parent. Despite the recalculation of the parental magma for the ultramafic zone, the modeling results of Higgins et al. (1997) are not changed demonstrably. Indeed, when the new composition is entered into the program MAGFOX, olivine is still the first phase that crystallizes, followed by pyroxene and spinel. Moreover, there is greater than 40% crystallization of olivine prior to the addition of a new phase, which is consistent with the observed stratigraphy (Sharkov et al., 1995; Higgins et al., 1997).

The parental magma for the ultramafic zone is LREE enriched and can be combined with a calculated dunite, with which it is in equilibrium (determined using the bulk D), to reproduce the observed trace-element variations in the samples (see Fig. 3). In fact, sample 200/444.7 can be produced by combining the calculated dunite with 22% of the parental liquid, and sample 248/190 can be produced by combining this dunite composition with 33% of the parental liquid. The percentage of parental liquid added is roughly the same as the modal abundance of intercumulus phases in each of these samples (i.e., 25% and 34% for samples 200/444.7 and 248/190, respectively). A "spidergram" (Sun and McDonough, 1989) of these calculated values is shown in Figure 5. In general, these other trace elements support the REE data. Note, however, that Sr, Zr, and Hf are enriched in the parental melt relative to the samples. This reflects the fact that the border-group sample (28/223) used to calculate the parent magma is slightly enriched in these elements.

The enrichment of sample 28/223 in Zr and Hf may be a result of the presence of an oxide phase such as chromite or ilmenite. Chromite has D values > 0.2, and ilmenite has D values > 1, for both of these elements (Table 3). Indeed, sample 28/223 contains 4 wt% chromite. Using a mass-balance approach, 4 wt% chromite was taken out, and the liquid was recalculated. This did not, however, affect the Zr and Hf levels demonstrably. The high D values for ilmenite indicate that relatively minor amounts could influence the Zr and Hf abundances in the calculated liquid. No ilmenite was found to be present in 28/223 petrographically, however, and a CIPW-norm calculation gives weight percentage values of < 1. Regardless, even if two percent ilmenite is assumed to have fractionated from the liquid (and this is generous since the largest amount of ilmenite observed in samples from either portion of the BLI is only

TABLE 3. Mineral/Melt Partition Coefficients

Element	Oliv[1]	Augite[2]	Opx[1]	Plag[1]	Spinel[3]	Ilmenite[6]
Sc	0.27	0.808	0.83[9]	0.0071	1.5	0.55
V	0.039	1.81	1	2.24[10]	38[7]	
Cr	3	1.66	2.6	0.0332	129[7]	
Co	5	1.2[1]	0.68[9]	0.0202	2.55[7]	
Ni	30	2.5[1]	1.3[9]	0.01	5.9[7]	
Cu[16]	0.12	0.57	0.21	0.11	0.098	
Rb	0.0001	0.026[11]	0.004[12]	1.75	0.0005	
Sr	0.0001	0.157	0.0034	1.61	0.0005	
Y	0.021	0.67[13]	0.19	0.044[12]	0.01	
Zr	0.008	0.195	0.021	0.0128	0.38	
Nb	0.0001	0.0081	0.027	0.005	0.01	
Ba	0.0001	0.0058	0.0063[13]	0.811	0.0005	0.005
La	0.0001	0.0515	0.0019	0.0418	0.029	0.029
Ce	0.0001	0.108	0.0035	0.0302	0.038	0.038
Nd	0.0001	0.277	0.013	0.021[11]	0.053	
Sm	0.0006	0.462	0.063	0.017	0.064	0.053
Eu	0.0007	0.458	0.059	0.166	0.061	0.02
Gd	0.001	[0.54]	0.069	[0.04]	[0.068]	
Tb	0.002	[0.6]	0.16	0.0095	0.078[8]	
Dy	0.003	0.711	0.15	[0.009]	[0.078]	
Ho	0.005	0.792[15]	0.3	[0.0084]	[0.078]	
Er	0.008	0.66	0.24	[0.0078]	[0.077]	
Tm	0.022	[0.63]	0.48	[0.0073]	[0.077]	
Yb	0.019	0.633	0.39	0.0065	0.39	0.39
Lu	0.03	0.623	0.67	0.0068	0.0213[8]	0.47
Hf	0.013	0.223	0.19[9]	0.0128	0.38	1.817

References: 1 = McKay (1986); 2 = Hauri et al. (1994); 3 = Dunn and Senn (1994); 4 = Phinney and Morrison (1990); 5 = McKenzie and O'Nions (1991); 6 = derived from Table 3 of Neal et al. (1989); 7 = Irving (1978); 4 = Nagasawa et al. (1980); 9 = estimated from Weill and McKay (1975); 10 = estimated from Dunn and Senn (1994); 11 = calculated using Rb/Sr of McKenzie and O'Nions (1991); 12 = calculated using Rb/Sr of Arth (1976); 13 = estimated from McKenzie and O'Nions (1991); 14 = calculated using Nd/Sm of Arth (1976); 15 = calculated using Ho/Er of Nicholls and Harris (1980); brackets represent D values determined by extrapolation from measured values of other REEs; 16 = from Ewart and Griffin (1994); 17 = estimated from Drake and Weill (1975). Many of the K_d values for spinel were taken from Table 3 of Neal et al. (1989).

about one percent), the observed Zr and Hf enrichments of the calculated liquid cannot be erased. Although we cannot state with certainty why this enrichment exists in sample 28/223, this is the reason for the high Zr and Hf in the calculated parental liquid.

Calculated parental liquids for the gabbronorite zone

No chilled-margin sample analyzed during this study is representative of the parental magma(s) of the gabbronorite zone. Thus, the parent composition had to be estimated on the basis of trace-element abundances in the samples. To accomplish this task, whole-rock trace-element concentrations were combined with bulk distribution coefficients, calculated from modal analyses and D values (Table 3), in order to estimate the liquids in equilibrium with each of the samples (Fig. 6). All of the calculated liquids are LREE enriched, with depleted HREE giving the patterns a rather steep negative slope. The calculated liquid for sample 354/279 is more LREE depleted than are the other calculated melts, which is not unexpected since the sample itself is extremely LREE depleted (see Fig. 4). Note also that the calculated liquid for sample 353/140 is more LREE enriched than those for the other samples, consistent with the earlier observation that this rock is anomalous. Sr abundances are relatively low in the calculated liquids (see Fig. 7), which primarily reflects the presence of plagioclase and augite in the samples (i.e., D values for Sr are 1.61 and 0.16, respectively, for these minerals). As expected, Sr abundances increase in

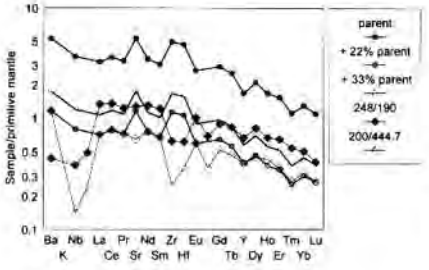

FIG. 5. Spidergram, showing various elements with increasing incompatibility (from right to left) relative to primitive mantle (Sun and McDonough, 1989), for the two parental-magma samples from the ultramafic zone. Also shown are various combinations of the parent magma and a calculated dunite (see text). Note that the model dunite + 22% parental-liquid ~ sample 200/444.7 and the dunite + 33% parental-liquid ~ sample 248/190.

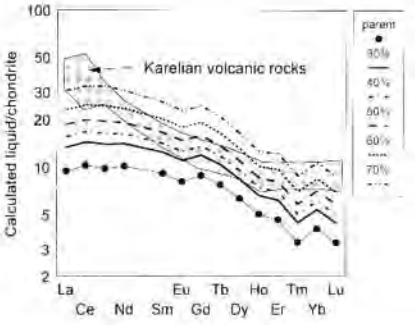

FIG. 6. Chondrite-normalized REE plot comparing the ultramafic-zone parental magma at various stages of crystallization with early Proterozoic Karelian volcanic rocks (shaded field) (Bogatikov, 1988).

the samples with increasing weight percentage plagioclase and augite. Nb is enriched in the liquids, and this is likely because it has very low D values (i.e., all are < 0.03) (Table 3) for the main cumulus phases (augite, plagioclase, orthopyroxene). The low Ba values in the calculated liquids reflect a D of 0.8 for plagioclase. Finally, the high Zr and Hf values for the calculated liquid for sample 353/140 may reflect crustal contamination. This idea is considered in detail below.

Magma Origins and Evolution

Calculated parental magmas for the ultramafic and gabbronorite zones of the Burakovsky layered intrusion are indicative of widespread magmatic activity in the eastern Baltic Shield in the early Proterozoic. The origins and evolution of these magmas are considered below.

Evidence for origin of the ultramafic zone

Samples from the ultramafic zone are LREE enriched and HREE depleted. These types of REE patterns are not uncommon for layered mafic intrusions of early Proterozoic age. Indeed, Lambert and Simmons (1987) recognized similar patterns in samples from the Ultramafic Series of the Stillwater Complex. They suggested that the parental magmas of the Stillwater Ultramafic Series, which they termed U-type, were characterized by $(Ce/Yb)_n$ ratios of 8 to 18, $(Nd/Sm)_n$ ratios of 1.6 to 2.0, and $(Dy/Yb)_n$ ratios of 1.7 to 1.9. In contrast, the parental magma calculated for the ultramafic zone of the BLI has a $(Ce/Yb)_n$ ratio of 2.6, a $(Nd/Sm)_n$ ratio of 1.1, and a $(Dy/Yb)_n$ of 1.6. These data indicate that the BLI parental magma was neither as LREE enriched as the U-type parent magmas of Lambert and Simmons (1987), nor as HREE depleted. However, Papike et al. (1995) performed secondary-ion mass-spectrometry (SIMS) analyses on orthopyroxene cores from the Stillwater Complex and determined that the LREE concentrations reported by Lambert and Simmons (1987) were too high. They believed this to be the result of the presence of one or more contaminating phases (e.g., plagioclase, augite) in the orthopyroxene mineral separates used by Lambert and Simmons (1987) for isotope-dilution analyses. Parental liquids, determined with the data of Papike et al. (1995), have $(Ce/Yb)_n$ ratios of 2.9 to 13.8, $(Nd/Sm)_n$ ratios of 0.8 to 1.3, and $(Dy/Yb)_n$ ratios of 1.1 to 1.9. These calculated liquids are similar to the REE characteristics of the parent magma calculated for the ultramafic zone of the BLI (see Fig. 3). Note, however, that the BLI parental magma plots at the least-abundant REE portion of the U-type parental magma field. Regardless, the important observation to be made here is that the REE patterns for the parental magma of the ultramafic zone of the BLI and that of the

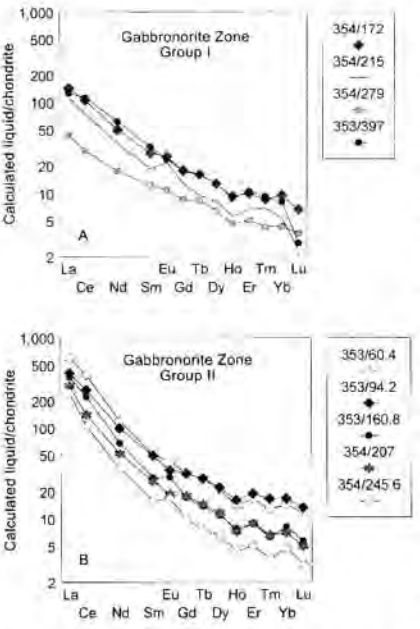

FIG. 7. Chondrite-normalized REE plots showing the two groups of parental magmas for the gabbronorite zone. A. Group I. B. Group II. Note the greater LREE enrichment in Group-II magmas as opposed to those of Group I.

Stillwater ultramafic rocks are both LREE enriched to similar degrees. This suggests that they may have formed under similar processes.

Lambert and Simmons (1987) proposed that the LREE enrichment of the U-type magma for the Stillwater Complex may have been caused by partial melting of an upper mantle containing veins enriched in LREE. The HREE characteristics of the U-type magma were explained by the presence of residual garnet throughout the melting process in the mantle (Lambert and Simmons, 1987). They further proposed that the melting of the source was a multi-stage, dynamic process. The similarity of the REE patterns for the BLI parent to the U-type parent of the Stillwater indicates that a comparable explanation may be offered. One problem, however, involves the multi-stage, dynamic, partial-melting model proposed by Lambert and Simmons (1987). Multi-stage, dynamic, partial melting of a garnet-bearing source should produce REE patterns that fan out from Yb, with early melts showing the largest enrichment in LREE, followed by progressively lower REE abundances in subsequent liquids (Loferski et al., 1994). In the ultramafic zone of the BLI, the REE patterns are subparallel (see Fig. 3), suggesting formation through simple fractional crystallization of a single melt, rather than as a product of multi-staged, dynamic, partial melting.

It can be argued that metasomatism is another mechanism that explains the origin of the LREE-enriched and HREE-depleted signatures in the parent magma of the ultramafic zone. It has been suggested as an explanation for similar REE characteristics determined for samples from the Stillwater Complex (Loferski et al., 1994). Metasomatic fluids normally are enriched in LREE relative to HREE, primarily because the HREE are slightly more compatible. As such, the interaction of these fluids with a source region would result in LREE enrichment. In addition, partial melts of this LREE-enriched source would have REE characteristics similar to those of the BLI magmas. Based upon this reasoning, metasomatism seems the most likely mechanism for enriching the mantle source region.

An origin proposed for the ultramafic zone, on the basis of major-element data (Higgins et al., 1997), involves an approach initially used to describe the petrogenesis of the Muskox Intrusion (Irvine and Smith, 1967; Irvine, 1970). This model entails the repeated addition of undifferentiated magma during accumulation. The residual magma is "flushed" from the system (effectively pushed out) by each addition of new magma. It was suggested in Higgins et al. (1997), on the basis of similar ages (i.e., 2500 ± 70 Ma versus 2449 ± 1.1 Ma for the BLI), that the Karelian volcanic fields that surround the BLI may be products of this "flushing." This idea can be evaluated more carefully by comparing chondrite-normalized REE plots for a suite of early Proterozoic Karelian komatiites (Bogatikov, 1988) with calculated liquids for the ultramafic zone (Fig. 6). It is apparent from Figure 6 that these volcanic rocks are related neither to the calculated parent liquid of the ultramafic zone nor to various values of F (i.e., the fraction of melt remaining) for this liquid. That is, the Karelian rocks are more enriched in LREE and are less depleted in the HREE rela-

tive to the ultramafic-zone samples. On the basis of these data, it can be concluded that the early Proterozoic Karelian volcanic rocks are not related to the episode of magmatism that produced the ultramafic zone of the BLI. This does not imply that there are no volcanic rocks in Karelia related to this magmatism, but that none have been reported to date.

REE evidence for origin of the gabbronorite zone

Samples from the gabbronorite zone have REE patterns with negative slopes (see Fig. 4), implying that, as with the ultramafic zone, they crystallized from a magma that was LREE enriched. The question that should be considered next is whether the gabbronorite zone crystallized from one single magma or from several. If the gabbronorite zone represents the crystallization product of a single magma, then the chondrite-normalized REE patterns for these liquids should be parallel, and there should be increasing REE abundances upward through the section. This results from the fact that the mineral-melt partition coefficients for the REE in the major cumulus minerals of this zone (e.g., augite, orthopyroxene, plagioclase) all are less than one (Table 3). However, the abundances of REE in samples from the gabbronorite zone are inconsistent with simple fractional crystallization from a single magma. In fact, there are at least two different parent magmas for the gabbronorite zone and these are here denoted as Group I and Group II. These two groups delineate calculated liquids with similar REE characteristics for samples from the lower and upper portions, respectively.

Parental liquids for samples from Group I are characterized by $(La/Nd)_n$ ratios ranging from 2.1 to 3.2. In contrast, Group-II parental melts are from higher stratigraphic levels, and have $(La/Nd)_n$ ratios ranging from 4.1 to 6.9. In addition, Group-I liquids have $(Ce/Yb)_n$ ratios of 6.9 to 13.9, $(Nd/Sm)_n$ ratios of 1.4 to 1.9, and $(Dy/Yb)_n$ ratios of 1.3 to 1.6. Group-II liquids have $(Ce/Yb)_n$ ratios ranging from 15.8 to 27.3, $(Nd/Sm)_n$ ratios of 2.0 to 2.4, and $(Dy/Yb)_n$ ratios of 1.3 to 1.7. It is proposed here, on the basis of these REE characteristics, that the lower subzone of the gabbronorite zone should be further subdivided into an upper and lower part.

As mentioned above, the REE abundances of samples formed from a single magma should become more enriched with increasing fractionation. It is apparent from Figure 7 that Group II is considerably more enriched in the LREE than is Group I (i.e., La is about 2 to 10 times more abundant). Chondrite-normalized REE patterns for Group-II liquids all are subparallel to parallel, and the most enriched liquid occurs at the highest stratigraphic level. These characteristics suggest that Group-II samples are fractionally crystallized derivatives of one parent magma. Group-I liquids, with the exception of 354/279, also have subparallel to parallel chondrite-normalized REE patterns. The liquid for sample 354/279 has a flatter LREE pattern, which suggests that it was influenced by some additional process. This sample will be considered in more detail below. The calculated liquid for 353/397 is more enriched in the REE than are the liquids for samples from higher in the sequence. It is possible that there may have been a pulse of new material following crystallization of sample 353/397. This also is supported by the major-element chemistry, in which the X_{Mg} changes from 0.77 to 0.81 from sample 353/397 to sample 354/279, respectively (Higgins et al., 1997).

Sample 353/140 has a REE pattern that is distinctly different from the other samples of the gabbronorite zone (see Fig. 4). Indeed, the parental liquid calculated from sample 353/140 has a $(Ce/Yb)_n$ ratio of 40.4, a $(Nd/Sm)_n$ ratio of 2.8, and a (Dy/Yb) ratio of 1.7, all of which are higher than values determined for liquids in equilibrium with the other samples. Moreover, this liquid also has much higher Zr and Hf values than the other gabbronorite-zone liquids (Fig. 8). One possible reason for the low HREE values could be the source region for this liquid; perhaps sample 353/140 crystallized from a liquid that was derived from a garnet-rich source, which would account for the HREE-depleted signature. However, there is no evidence that suggests why the source region for this sample would be so much different from that for the other samples of the gabbronorite zone. Another possible explanation is that the parental liquid for sample 353/140 may have been contaminated by Archean crust. In fact, using a simple mass-balance calculation, the observed REE patterns and the high Zr and Hf values in this melt can be produced through

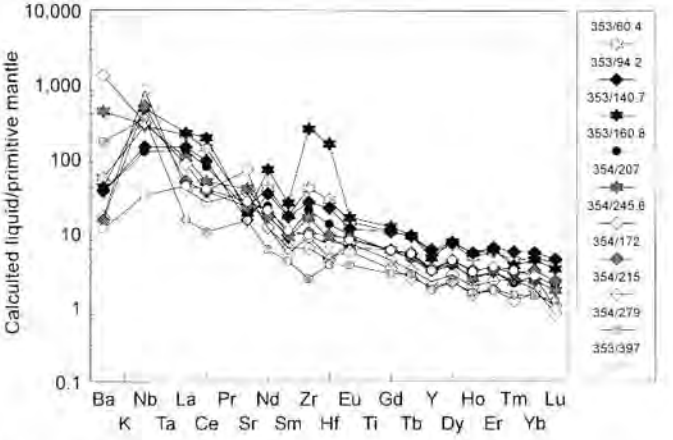

FIG. 8. A spidergram (Sun and McDonough, 1989) showing the calculated liquids from the gabbronorite zone, normalized to primitive mantle. Note the high abundances of Zr and Hf in the parent liquid for sample 353/140.

contamination with 5 to 10% of a typical felsic Archean crustal rock (Rudnick and Fountain, 1995).

Enriched Character of the Mantle during the Late Archean

We have indicated above that the volcanic rocks that are coeval with the BLI have REE abundances and patterns that are distinct from the calculated liquids of either the ultramafic or the gabbronorite zone. However, sparse Nd-isotopic data suggest that the Karelian volcanics are also derived from old, enriched mantle (Pukhtel et al., 1991). The differences in LREE enrichment between the layered intrusions and the volcanics may be the result of different degrees of partial melting or heterogeneities in the enriched mantle source. Similarly LREE-enriched volcanic rocks in the northeastern Baltic Shield (Melezhik and Sturt, 1994) indicate that this enriched mantle persisted laterally for hundreds of kilometers beneath the eastern Baltic Shield. Moreover, layered intrusions of the northeastern Baltic Shield (e.g., the Olanga Complex, the Monchegorsk, the Pana Tundra), like the BLI, tend to be characterized by LREE-enriched patterns (Melezhik and Sturt, 1994).

The LREE-enriched nature of the proposed parental magma for the ultramafic zone of the BLI suggests that it may have formed from partial melting of a large-ion-lithophile element (LILE)-enriched mantle source. Alternatively, these LREE characteristics could be a product of contamination of the parent magma by LREE-enriched crustal rocks en route to the BLI magma chamber. However, the ϵ_{Nd} of the BLI is -2.0 (Mitrofanov and Torokhov, 1994), suggesting that significant crustal contamination did not occur (e.g., typical Archean gneisses have ϵ_{Nd} values of -30 to -40) (Collerson and McCulloch, 1982). Moreover, layered intrusions of the Baltic Shield, of similar age to the BLI, have uniformly low ϵ_{Nd} values (from 2.44 to 2.50 Ga) ranging from -1.8 to -2.2 (Burakovsky, Federova-Pansky, Penikat, Mt. Generalskaya, Imandra, and Monchegorsk) (Fig. 9). If crustal contamination were the main cause of the LREE-enriched characteristics of these intrusions, then one would expect greater variability in the ϵ_{Nd} values over such a large region (i.e., the Baltic Shield). Although there is evidence of localized contamination of these magmas (Amelin et al., 1995), Sr-isotopic data on several of these intrusions have yielded initial ratios consistent with mantle derivation (Mitrofanov and Balashov, 1990). Furthermore,

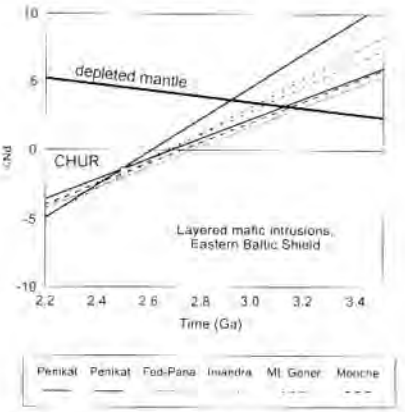

FIG. 9. Nd-isotopic evolution diagram for several early Proterozoic layered mafic intrusions (Penikat, Federova-Pansky, Imandra, Mt. Generalskaya, and Monchegorsk plutons) in the eastern Baltic Shield. Note that the evolution lines converge at 2.47 to 2.50 Ga and cross the depleted-mantle evolution line at 2.9 to 3.2 Ga.

the tight range of initial Nd-isotopic ratios for these intrusions effectively rules out contamination as a major, controlling factor. Thus, the negative ϵ_{Nd} values of the BLI are likely a product of derivation of the BLI parent magma(s) from a mantle source that was enriched in LREE for a significant period of time, rather than a result of crustal contamination.

These intrusions yield depleted-mantle model ages from 2.9 to 3.2 Ga (Fig. 9). Because melts of a source that consists mostly of mafic minerals, as does the Earth's mantle, will nearly always be more LREE enriched (i.e., have a lower Sm/Nd ratio) than the source, these model ages give the minimum age of separation of the enriched mantle from a continuously depleting upper-mantle reservoir. Thus, we can state with some confidence that the source for this widespread magmatic event during the early Proterozoic was old, enriched mantle that may have been created prior to 3.2 Ga.

Finally, these LREE-enriched characteristics are not confined to early Proterozoic layered intrusions of the Baltic Shield. Indeed, similar REE patterns have been observed for Archean-Proterozoic intrusions in other parts of the world (e.g., the Stillwater and Bushveld complexes) (Lambert and Simmons, 1987 and Sharpe and Hulbert, 1985, respectively), which suggests that the LREE enrichment that affected the mantle beneath the Baltic Shield may not have been a localized event, but perhaps occurred on a worldwide scale.

Summary and Conclusions

Trace-element abundances in whole rocks from the ultramafic and gabbronorite zones of the BLI have defined certain geochemical characteristics that must be explained in any interpretation of the petrogenesis of this large pluton. Samples from the ultramafic zone are LREE enriched, with $(Ce/Yb)_n$ ratios of 2.2 to 2.5, $(Nd/Sm)_n$ ratios of 1.1 to 1.2, and $(Dy/Yb)_n$ ratios of 1.3 to 1.6. These REE characteristics are consistent with the ultramafic zone having formed from an LREE-enriched magma. It is suggested that the chilled margin of the BLI, when recalculated to account for excess olivine, represents the parental magma of the ultramafic zone. This magma has the following geochemical characteristics: a $(Ce/Yb)_n$ ratio of 2.6, a $(Nd/Sm)_n$ ratio of 1.1, and a $(Dy/Yb)_n$ ratio of 1.6. The LREE enrichment in the calculated parent magma suggests either that the mantle source region was LREE enriched or that the liquid was contaminated by LREE-enriched crustal rocks en route to the BLI magma chamber. Negative ϵ_{Nd} values for rocks from the BLI are most consistent with a mantle source region that was LREE enriched for a significant period of geologic time prior to the partial melting episode that produced the parental magma(s). This enrichment of the mantle source region likely resulted from metasomatism.

Samples from the gabbronorite zone are LREE enriched and are characterized by $(Ce/Yb)_n$ ratios of 2.1 to 6.8, $(Nd/Sm)_n$ ratios of 1.1 to 1.5, and $(Dy/Yb)_n$ ratios of 1.2 to 1.7. Liquids in equilibrium with these samples have $(Ce/Yb)_n$ ratios of 11 to 27, $(Nd/Sm)_n$ ratios of 1.8 to 2.4, and $(Dy/Yb)_n$ ratios of 1.3 to 1.7. At least two different parental magmas were involved in the formation of the lower subzone of the gabbronorite zone, as evidenced by the variation in REE for calculated parental liquids for samples of different stratigraphic height. Group-I samples, from the lower portion of the gabbronorite zone, are characterized by paren-

tal liquids with (La/Nd) ratios of 2.1 to 3.2, $(Ce/Yb)_n$ ratios of 6.9 to 13.9, and $(Dy/Yb)_n$ ratios of 1.3 to 1.6. In contrast, Group-II samples, from the upper part of the gabbronorite zone, are characterized by $(La/Nd)_n$ ratios of 4.1 to 6.9, $(Ce/Yb)_n$ ratios of 15.8 to 27.3, and $(Dy/Yb)_n$ ratios of 1.3 to 1.7.

The similarities in REE characteristics between the parent liquid of sample 354/279 (an olivine pyroxenite from the lower part of the gabbronorite zone) and sample 28/223 (thought to represent a liquid composition for the ultramafic zone) suggest that the olivine pyroxenite/harzburgite layers that occur in the lower portions of the gabbronorite zone likely crystallized from liquids derived from the ultramafic zone. This provides evidence that the source of magma for the ultramafic zone was not exhausted after its formation, but continued periodically to intrude pulses of material into the gabbronorite zone.

The REE characteristics of the ultramafic and gabbronorite zones are consistent with derivation from a LREE-enriched source. Moreover, volcanic rocks of similar age in Karelia and the northeastern Baltic Shield are similarly LREE enriched. No volcanic rocks that have been analyzed to date, however, appear to be related to the magmatism that formed the BLI. This implies that the magma that crystallized to form the BLI either never made it to the surface or did so but later was eroded away. Despite this, the fact that the majority of early Proterozoic-aged rocks from the Baltic Shield have LREE-enriched signatures indicates that the mantle during this time likely was LREE enriched. Moreover, the narrow range in ϵ_{Nd} values for other early Proterozoic layered intrusions of this region (e.g., ϵ_{Nd} values ranging from −1.8 to −2.2) suggests that crustal contamination was not a major factor in producing the observed LREE enrichments. Finally, intrusions of similar ages occurring in other cratons (e.g., the Stillwater Complex, the Bushveld Complex) display these same types of LREE-enriched patterns. This may indicate that the LREE enrichment was not a localized event, but instead occurred on a worldwide basis.

Acknowledgments

We wish to thank our friends and colleagues at the Karelian Geological Expedition, Petrozavodsk, Russia for their hospitality and helpful discussions during the senior author's stay, and for supplying the samples used in this study. This research was partially supported by NSF research grants ECS 92-14596 (to CRN) and EAR 93-04053 (to LAT).

REFERENCES

Alapieti, T. T., Filen, B. A., Lahtinen, J. J., Lavrov, M. M., Smolkin, V. F., and Voitsekhovsky, S. N., 1990, Early Proterozoic layered intrusions in the northeastern part of the Fennoscandian Shield: Mineral. Petrol., v. 42, p. 1–22.

Amelin, Y. V., Heaman, L. M., and Semenov, V. S., 1995, U-Pb geochronology of layered mafic intrusions in the eastern Baltic Shield: Implications for the timing and duration of Paleoproterozoic continental rifting: Precamb. Res., v. 75, p. 31–46.

Arth, J. G., 1976, Behavior of trace elements during magmatic processes—a summary of theoretical models and their applications: Jour. Res., U.S. Geol. Surv., v. 4, p. 41–47.

Balashov, Y. Z., Bayanova, T. B., and Mitrofanov, F. P., 1993, Isotope data on the age and genesis of layered basic-ultrabasic intrusions in the Kola Peninsula and northern Karelia, northeastern Baltic Shield: Precamb. Res., v. 64, p. 197–205.

Bogatikov, O. A., 1988, Komatiites and high-magnesium volcanics in the early Precambrian of the Baltic Shield: Leningrad, Nauka Press (in Russian).

Carlson, R. W., and Irving, A. J., 1994, Depletion and enrichment history of subcontinental lithospheric mantle: An Os, Sr, Nd and Pb isotopic study of xenoliths from the northwestern Wyoming craton: Earth Planet. Sci. Lett., v. 124, p. 457–472.

Collerson, K. D., and McCulloch, M. T., 1982, The origin and evolution of Archean crust, as inferred from Nd, Sr and Pb isotopic studies in Labrador [abs.]: Abs. Fifth Int. Conf. Geochron. Cosmochron. Isotope Geol., Nikko, Japan, p. 61–62.

Collerson, K. D., and Sheraton, J. W., 1986, Age and geochemical characteristics of a mafic dyke swarm in the Archean Vestfold Block, Antarctica: Inferences about Proterozoic dyke emplacement in Gondwana: Jour. Petrol., v. 27, p. 853–886.

Dalpé, C., and Baker, D. R., 1993, The importance of amphibole and mica in the generation of alkali basaltic suites [abs.]: Geol. Assoc. Canada—Mineral. Assoc. Canada, Prog. Abs., v. 18, p. A22.

Drake, M. J., and Weill, D. F., 1975, The partition of Sr, Ba, Ca, Y, Eu^{2+}, Eu^{3+} and other REE between plagio-

clase feldspar and magmatic silicate liquid: An experimental study: Geochim. et Cosmochim. Acta, v. 39, p. 689–712.

Dunn, T., and Sen, C., 1994, Mineral/matrix partition coefficients for orthopyroxene, plagioclase, and olivine in basaltic to andesitic systems: A combined analytical and experimental study: Geochim. et Cosmochim. Acta, v. 58, p. 717–733.

Ewart, A., and Griffin, W. L., 1994, Application of proton-microprobe data to trace-element partitioning in volcanic rocks: Chem. Geol., v. 117, p. 251–284.

Gorbatschev, R., and Bogdanova, S., 1993, Frontiers in the Baltic Shield: Precamb. Res., v. 64, p. 3–21.

Hauri, E. H., Wagner, T. P., and Grove, T. L., 1994, Experimental and natural partitioning of Th, U, Pb and other trace elements between garnet, clinopyroxene and basaltic melts: Chem. Geol., v. 117, p. 149–166.

Heaman, L. M., 1988, A precise U-Pb zircon age for a Hearst Dyke [abs.]: Geol. Assoc. Canada, v. 13, p. A53.

Heaman, L. M., and Tarney, J., 1989, U-Pb baddleyite ages for the Scourie dyke swarm, Scotland: Evidence of two distinct intrusion events: Nature, v. 340, p. 705–708.

Higgins, S. J., 1996, Petrology and geochemistry of the early Proterozoic Burakovsky layered intrusion, southern Karelia, Russia: Unpubl. M.Sc. thesis, Univ. of Tennessee, 112 p.

Higgins, S. J., Snyder, G. A., Mitchell, J. N., Taylor, L. A., Sharkov, E. V., Bogatikov, O. A., Grokhovskaya, T. L., Chistyakov, A. V., Ganin, V. A., and Grinevich, N. G., 1997, Petrology of the early Proterozoic Burakovsky layered intrusion, southern Karelia, Russia: Part I. Mineral and whole-rock major-element chemistry: Canad. Jour. Earth Sci. (in press).

Irvine, T. N., 1970, Crystallization sequences in the Muskox Intrusion and other layered intrusions: Geol. Soc. Amer. Spec. Publ., v. 1, p. 441–476.

———, 1980, Magmatic infiltration metasomatism, double diffusive fractional crystallization and adcumulus growth in the Muskox intrusion and other layered intrusions, *in* Hargraves, R. B., ed., Physics of magmatic processes: Princeton, NJ, Princeton Univ. Press, p. 325–384.

Irvine, T. N., and Smith, C. H., 1967, The ultramafic rocks of the Muskox intrusion, Northwest Territories, Canada, *in* P. J. Wyllie, ed., Ultramafic and related rocks: New York, John Wiley and Sons, p. 38–49.

Irving, A. J., 1978, A review of experimental studies of crystal/liquid trace element partitioning: Geochim. et Cosmochim. Acta, v. 42, p. 743–770.

Koptev-Dvornikov, E. V., 1995, Usage of the convective-cumulative model for simulation of the layered intrusions crystallization: Proceedings of the Int. Field Conf. and Symposium on Petrology and Metallogeny of Volcanic and Intrusive Rocks of the Midcontinent Rift System: Duluth, MN, IGCP Project 336, 85–86.

Krogh, T. E., Davis, D. W., and Corfu, F., 1984, Precise U-Pb zircon and baddeleyite ages for the Sudbury area, *in* Pye, E. G., Naldrett, A. J., and Giblin, P. E., eds., The geology and ore deposits of the Sudbury structure: Toronto, Ontario Geol. Surv. Spec. v. 1, p. 431–446.

Lambert, D. D., and Simmons, E. C., 1987, Magma evolution in the Stillwater Complex, Montana: I. Rare-earth element evidence for the formation of the Ultramafic Series: Amer. Jour. Sci., v. 287, p. 1–32.

Loferski, P. J., Arculus, R. J., and Czamanske, G. K., 1994, Rare-earth element evidence for the petrogenesis of the Banded Series of the Stillwater Complex, Montana, and its anorthosites: Jour. Petrol., v. 35, p. 1623–1649.

McClay, K. R., and Campbell, I. H., 1976, The structure and shape of the Jimberlana intrusion, Western Australia, as indicated by an investigation of the Bronzite Complex: Geol. Mag., v. 113, p. 129–139.

McKay, G. A., 1986, Crystal/liquid partitioning of REE in basaltic systems: Extreme fractionation of REE in olivine: Geochim. et Cosmochim. Acta, v. 50, p. 69–79.

McKenzie, D., and O'Nions, R. K., 1991, Partial melt distributions from inversion of rare earth element concentrations: Jour. Petrol., v. 29, p. 625–679.

Melezhik, V. A., and Sturt, B. A., 1994, General geology and evolutionary history of the early Proterozoic Polmak-Pasvik-Pechenga-Imandra/Varzuga-Ust' Ponoy Greenstone Belt in the northeastern Baltic Shield: Earth Sci. Rev., v. 36, p. 205–241.

Menzies, M. A., 1990, Archacan, Proterozoic, and Phanerozoic lithospheres, *in* Menzies, M. A., ed., Continental mantle: Oxford, UK, Clarendon Press, p. 67–86.

Menzies, M. A., and Murthy, V. R., 1980, Enriched mantle: Nd and Sr isotopes in diopsides from kimberlite nodules: Nature, v. 283, p. 634–636.

Mitrofanov, F. P., and Balashov, Yu. A., eds., 1990, Geochronology and genesis of layered basic intrusions, volcanites, and granite-gneisses of the Kola peninsula: Apatity, Kola Science Center, 48 p.

Mitrofanov, F. P., and Torokhov, M., eds., 1994, Guide to the pre-symposium field trip: Kola belt of layered intrusions: Apatity, Kola Science Center, 109 p.

Nagasawa, H., Schreiber, H. D., and Morris, R. V., 1980, Experimental mineral/liquid partition coefficients of the rare earth elements (REE), Sc and Sr for perovskite, spinel, and melilite: Earth Planet. Sci. Lett., v. 46, p. 431–437.

Neal, C. R., Taylor, L. A., Schmitt, R. A., Hughes, S. S., and Lindstrom, M. M., 1989, High alumina (HA) and very high potassium (VHK) basalt clasts from Apollo 14 breccias, Part 2—Whole-rock geochemistry: Further evidence for combined assimilation and fractional crystallization within the lunar crust: Proc. Lunar Planet. Sci. Conf., v. 19, p. 147–161.

Nicholls, I. A., and Harris, K. L., 1980, Experimental rare earth element partition coefficients for garnet, clinopyroxene and amphibole coexisting with andesitic and basaltic liquids: Geochim. et Cosmochim. Acta, v. 44, p. 287–308.

O'Brien, H. E., Irving, A. J., McCallum, I. S., and Thirlwall, M. F., 1995, Strontium, neodymium, and lead isotopic evidence for the interaction of post-subduction asthenospheric potassic mafic magmas of the Highwood Mountains, Montana, USA, with ancient Wyoming craton lithospheric mantle: Geochim. et Cosmochim. Acta, v. 59, p. 4539–4556.

Papike, J. J., Spilde, M. N., Fowler, G. W., and McCallum, I. S., 1995, SIMS studies of planetary cumulates: Orthopyroxene from the Stillwater Complex, Montana: Amer. Mineral., v. 80, p. 1208–1221.

Phinney, W. C., and Morrison, D. A., 1990, Partition coefficients for calcic plagioclase: Implications for Archean anorthosites: Geochim. et Cosmochim. Acta, v. 54, p. 1639–1654.

Pukhtel, I. S., Zhuravlev, D. Z., Kulikov, V. S., and Kulikova, V. S., 1991, Petrography and Sm-Nd age of komatiitic basalt in the Vetra belt, Baltic Shield: Geochem. Int., v. 28, p. 14–23.

Richardson, S. H., Erlank, A. J., and Hart, S. R., 1985, Kimberlite-borne garnet peridotite xenoliths from old enriched subcontinental lithosphere: Earth Planet. Sci. Lett., v. 75, p. 116–128.

Rudnick, R. L., and Fountain, D. M., 1995, Nature and composition of the continental crust: A lower crustal perspective: Rev. Geophys., v. 33, p. 267–309.

Scott-Smith, B. H., 1987, Greenland, *in* Nixon, P. H., ed., Mantle xenoliths: Chichester, UK, John Wiley and Sons, p. 23–32.

Sharkov, E. V., Bogatikov, O. A., Grokhovskaya, T. L., Chistyakov, A. V., Ganin, V. A., Grinevich, N. G., Snyder, G. A., and Taylor, L. A., 1995, Petrology and Ni-Cu-Cr-PGE mineralization of the largest mafic pluton in Europe: The Early Proterozoic Burakovsky Layered Intrusion, Karelia, Russia: Int. Geol. Rev., v. 37, p. 509–525.

Sharpe, M. R., and Hulbert, L. J., 1985, Ultramafic sills beneath the eastern Bushveld Complex: Mobilized suspensions of early lower zone cumulates in a parental magma with boninitic affinities: Econ. Geol., v. 80, p. 849–871.

Sheraton, J. W., and Black, L. P., 1981, Geochemistry and geochronology of Proterozoic tholeiite dykes of east Antarctica: Evidence from mantle metasomatism: Contrib. Mineral. Petrol., v. 78, p. 305–317.

Simmons, E. C., and Lambert, D. D., 1982, Magma evolution in the Stillwater Complex, Montana: A preliminary evaluation using REE data for whole-rocks and cumulate feldspars: Great Falls, MT, Montana Bureau of Mines Spec. Publ., v. 84, p. 91–106.

Sun, S.-S., and McDonough, W. F., 1989, Chemical and isotopic systematics of oceanic basalts: Implications for mantle compositions and processes, *in* Saunders, A. D., and Norry, M. J., eds., Magmatism in the ocean basins: London, Geol. Soc. London, Spec. Publ., v. 42, p. 313–345.

Wager, L. R., and Brown, G. M., 1967, Layered igneous rocks: San Francisco, Freeman and Company.

Wager, L. R., and Deer, W. A., 1939, Geological investigations in East Greenland. Pt. III. The petrology of the Skaergaard Intrusion, Kangerdlugssuaq, East Greenland: Meddr. Gronland, v. 105, no. 4, p. 1–352.

Wasson, J. T., and Kallemeyn, G. W., 1988, Compositions of chondrites: Phil. Trans. Roy. Soc. Lond., v. A325, p. 535–544.

Weill, D. F., and McKay, G., 1975, The partitioning of Mg, Fe, Sr, Ce, Sm, Eu, and Yb in lunar igneous systems and a possible origin of KREEP by equilibrium partial melting: Proc. Lunar Sci. Conf., v. 6, p. 1143–1158.

Wilson, A. H., and Prendergast, M. D., 1987, The Great Dyke of Zimbabwe—an overview, *in* Guidebook for the 5th Magmatic Sulfides Field Conf.: Harare, Geol. Soc. Zimbabwe, p. 23–55.